

# The S-wave topped meson

Jun-Hao Zhang<sup>1,2</sup>, Shuo Yang<sup>1,2,\*</sup> and Bing-Dong Wan<sup>1,2†</sup>

<sup>1</sup>*School of Physics and Electronic Technology,  
Liaoning Normal University, Dalian 116029, China*

<sup>2</sup> *Center for Theoretical and Experimental High Energy Physics,  
Liaoning Normal University, Dalian 116029, China*

## Abstract

Inspired by the recent observation of the near-threshold enhancement in top-quark pair production by CMS and ATLAS, we investigate the mass spectrum of S-wave topped meson which containing a single top quark, i.e.,  $t\bar{q}$ ,  $t\bar{c}$ , and  $t\bar{b}$ , in the framework of Bethe-Salpeter formalism. These states are expected to exhibit significantly enhanced lifetimes and correspondingly narrower decay widths compared to toponium, primarily because only a single top quark participates in the weak decay process. The numerical results indicate that the masses of topped mesons are close to the top-quark mass. For the  $t\bar{b}$  states, the  $1S$  state is approximately 5.08 GeV heavier than the top quark, while the  $2S$ ,  $3S$ , and  $4S$  states are about 5.37 GeV, 5.57 GeV, and 5.74 GeV heavier, respectively. For the  $t\bar{c}$  states, the corresponding mass differences are 1.90 GeV, 2.23 GeV, 2.45 GeV, and 2.60 GeV. The possible production and decay properties are also analyzed, which could be measured in LHC experiments.

---

\*Electronic address: [shuoyang@lnnu.edu.cn](mailto:shuoyang@lnnu.edu.cn)

†Electronic address: [wanbd@lnnu.edu.cn](mailto:wanbd@lnnu.edu.cn)

## I. INTRODUCTION

Because of its exceptionally large mass (172.76 GeV) and large decay width ( $1.42^{+0.19}_{-0.15}$  GeV) [1], the top quark decays on a timescale ( $\tau_t \approx 5 \times 10^{-25}$  s) that is far shorter than the characteristic QCD hadronization time ( $\tau_{had} \sim 1/\Lambda_{QCD} \approx 10^{-23}$  s). This hierarchy of timescales renders the top quark effectively difficult to hadronize, thereby giving it a uniquely singular status within the Standard Model and distinguishing it from all other quarks that inevitably form hadrons. This remarkable characteristic presents profound theoretical challenges and, at the same time, offers novel opportunities for deeper exploration in hadronic physics.

The top quark pair near threshold is produced copiously at the highly energetic Large hadron Collider(LHC), which provides an opportunity to explore the strong interaction in the presence of heavy quarks. Recently, both the CMS and ATLAS collaborations have reported a statistically significant excess in the  $\bar{t}t$  invariant-mass spectrum near threshold [2, 3], consistent with a pseudoscalar toponium state. Similar structures in earlier ATLAS and CMS datasets also support this interpretation [4, 5]. Inspired by the observation of this quasi-bound toponium state with a significance exceeding  $5\sigma$  [2, 3], a wide range of theoretical investigations has been carried out [6–31], including studies on toponium production and decay [25–28], and possible “topped” mesons and baryons [29–31]. In addition, it should be noted that numerous theoretical predictions had previously anticipated the existence of toponium [32–56].

In light of these developments, it is valuable to explore QCD phenomena involving top quarks, investigate whether analogous near-threshold structures can emerge in systems containing a single top quark, and anticipate further experimental tests. Unlike toponium, where both the production rate and resonance profile are dominantly shaped by short-distance QCD dynamics, the formation of topped mesons introduces an interplay between electroweak decay, light-quark binding, and potential nonperturbative enhancements. Although conventional potential-model analyses suggest that the top quark decays too rapidly to permit fully developed bound states, quasi-bound

or resonant configurations may still manifest as distortions in differential distributions, such as the invariant mass of the top–light-quark system or the angular correlations among top decay products.

Furthermore, the markedly reduced decay width expected for these single-top mesonic configurations implies that even modest binding effects could produce experimentally resolvable features, especially in precision measurements of single-top production channels. As the LHC and future colliders accumulate larger datasets, the improved sensitivity may enable the identification of subtle spectral anomalies or deviations from Standard Model expectations associated with such top–light-quark correlations. Relevant systematic theoretical studies will be essential for interpreting any observed excesses and for distinguishing genuine hadronic effects from higher-order electroweak or QCD radiative corrections.

Ultimately, the study of topped mesons provides a novel arena in which to test the boundary between perturbative and nonperturbative QCD in the presence of an unstable heavy quark. Should experimental signatures of these states be confirmed, they would constitute not only a new class of heavy–light hadrons but also a critical benchmark for our understanding of strong-interaction dynamics at the electroweak scale, thereby opening a new chapter in top-quark phenomenology.

In this work, we investigate the the mass spectrum of S-wave topped meson which containing a single top quark, i.e.,  $t\bar{q}$ ,  $t\bar{c}$ , and  $t\bar{b}$ , in the framework of Bethe-Salpeter (BS) formalism. The rest of the paper is organized as follows. After the introduction, a brief interpretation of BS equation and some primary formulas in our calculation are presented in Sec. II. We give the numerical analysis and results in Sec. III. In Sec. IV, possible production and decay modes of topped mesons are investigated. The last part is left for conclusions and discussions.

## II. BETHE-SALPETER EQUATION

In quantum field theory, the BS equation provides a fundamental, relativistically covariant framework for the description of two-body bound states [57]. The BS wave function of a quark–antiquark bound state is defined by the time-ordered vacuum-to-bound-state matrix element

$$\chi(x_1, x_2) = \langle 0 | T\{\psi(x_1) \bar{\psi}(x_2)\} | P \rangle, \quad (1)$$

where  $x_1$  and  $x_2$  denote the spacetime coordinates of the quark and antiquark, respectively,  $|P\rangle$  is the bound-state eigenvector with total four-momentum  $P$ , and  $T$  denotes the time-ordering operator. Eq. (1) serves as the starting point for the derivation of the BS equation in momentum space after Fourier transformation and the imposition of an appropriate interaction kernel.

The BS wave function in momentum space is defined through the Fourier transformation of the coordinate-space wave function,

$$\chi_P(q) = e^{-iP \cdot X} \int d^4x e^{-iq \cdot x} \chi(x_1, x_2), \quad (2)$$

where  $q$  denotes the relative four-momentum between the quark and the antiquark. The “center-of-mass” coordinate  $X$  and the “relative” coordinate  $x$  are defined as

$$X = \frac{m_1}{m_1 + m_2} x_1 + \frac{m_2}{m_1 + m_2} x_2, \quad x = x_1 - x_2, \quad (3)$$

with  $m_1$  and  $m_2$  being the masses of the quark and antiquark, respectively. Then the bound state BS equation in momentum space takes the form

$$S_1^{-1}(p_1)\chi_P(q)S_2^{-1}(-p_2) = i \int \frac{d^4k}{(2\pi)^4} V(P; q, k) \chi_P(k). \quad (4)$$

Here the fermion propagators are given by

$$S_i(\pm p_i) = \frac{i}{\pm \not{p}_i - m_i}, \quad (i = 1, 2), \quad (5)$$

and  $V(P; q, k)$  denotes the interaction kernel. The momenta of the quark and antiquark can be expressed as

$$p_i = \frac{m_i}{m_1 + m_2} P + Jq, \quad (6)$$

where  $J = 1$  for the quark ( $i = 1$ ) and  $J = -1$  for the antiquark ( $i = 2$ ). With the definitions

$$p_{iP} \equiv \frac{P \cdot p_i}{M}, \quad p_{i\perp}^\mu \equiv p_i^\mu - \frac{P \cdot p_i}{M^2} P^\mu, \quad (7)$$

the propagator  $S_i(Jp_i)$  can be decomposed as

$$-iJ S_i(Jp_i) = \frac{\Lambda_i^+(q_\perp)}{p_{iP} - \omega_i + i\epsilon} + \frac{\Lambda_i^-(q_\perp)}{p_{iP} + \omega_i - i\epsilon}, \quad (8)$$

where the projection operators are defined by

$$\begin{aligned} \Lambda_i^\pm(q_\perp) &\equiv \frac{1}{2\omega_i} \left[ \frac{\not{P}}{M} \omega_i \pm (\not{p}_{i\perp} + J m_i) \right], \\ \omega_i &\equiv \sqrt{m_i^2 - p_{i\perp}^2}. \end{aligned} \quad (9)$$

Under the instantaneous approximation, the interaction kernel in the center-of-mass frame can be written as

$$V(P; q, k) \Big|_{\vec{P}=0} \simeq V(q_\perp, k_\perp). \quad (10)$$

Accordingly, the BS equation can be reduced to

$$\chi_P(q) = S_1(p_1) \eta_P(q_\perp) S_2(-p_2), \quad (11)$$

with

$$\eta_P(q_\perp) = \int \frac{d^3 k_\perp}{(2\pi)^3} V(q_\perp, k_\perp) \varphi_P(k_\perp), \quad (12)$$

where the three-dimensional BS wave function is defined as

$$\varphi_P(q_\perp) \equiv i \int \frac{dq_P}{2\pi} \chi_P(q). \quad (13)$$

By introducing the projected components of the Salpeter wave function as

$$\varphi_P^{\pm\pm}(q_\perp) \equiv \Lambda_1^\pm(q_\perp) \frac{\not{P}}{M} \varphi_P(q_\perp) \frac{\not{P}}{M} \Lambda_2^\pm(q_\perp), \quad (14)$$

the three-dimensional BS wave function can be decomposed into its four components:

$$\varphi_P(q_\perp) = \varphi_P^{++}(q_\perp) + \varphi_P^{+-}(q_\perp) + \varphi_P^{-+}(q_\perp) + \varphi_P^{--}(q_\perp). \quad (15)$$

Correspondingly, the BS equation (11) can be decomposed into four coupled equations for the projected components:

$$(M - \omega_1 - \omega_2) \varphi_P^{++}(q_\perp) = \Lambda_1^+(q_\perp) \eta_P(q_\perp) \Lambda_2^+(q_\perp), \quad (16)$$

$$(M + \omega_1 + \omega_2) \varphi_P^{--}(q_\perp) = -\Lambda_1^-(q_\perp) \eta_P(q_\perp) \Lambda_2^-(q_\perp), \quad (17)$$

$$\varphi_P^{+-}(q_\perp) = \varphi_P^{-+}(q_\perp) = 0, \quad (18)$$

where  $\omega_i = \sqrt{m_i^2 + q_\perp^2}$  and  $\Lambda_i^\pm(q_\perp)$  are the projection operators defined in Eq. (9).

To solve the BS equation, a proper understanding of the interquark potential is essential. According to lattice QCD calculations, the potential for a heavy quark–antiquark pair in the static limit is well described by a long-range linear confining potential (Lorentz scalar  $V_S$ ) and a short-range one-gluon-exchange potential (Lorentz vector  $V_V$ ) [58–60]:

$$\begin{aligned} V(r) &= V_S(r) + \gamma_\mu \otimes \gamma^\mu V_V(r), \\ V_S(r) &= \lambda r \frac{1 - e^{-\alpha r}}{\alpha r}, \\ V_V(r) &= -\frac{4}{3} \frac{\alpha_s(r)}{r} e^{-\alpha r}. \end{aligned} \quad (19)$$

Here, the factor  $e^{-\alpha r}$  is introduced not only to avoid infrared divergence but also to incorporate the color-screening effects of dynamical light-quark pairs on the “quenched” potential [61].

The potentials in momentum space are given by

$$\begin{aligned} V(\vec{p}) &= (2\pi)^3 V_S(\vec{p}) + \gamma_\mu \otimes \gamma^\mu (2\pi)^3 V_V(\vec{p}), \\ V_S(\vec{p}) &= -\left(\frac{\lambda}{\alpha}\right) \delta^3(\vec{p}) + \frac{\lambda}{\pi^2} \frac{1}{(\vec{p}^2 + \alpha^2)^2}, \\ V_V(\vec{p}) &= -\frac{2\alpha_s}{3\pi^2} \frac{1}{\vec{p}^2 + \alpha^2}. \end{aligned} \quad (20)$$

Here,  $\alpha_s$  is the strong coupling constant, and the parameters  $\alpha$  and  $\lambda$  characterize the potential. Ref. [35] indicates that the mass splitting between the singlet and triplet states is entirely negligible due to the large top-quark mass, i.e.,

$$M_{0-}(n, {}^1S_0) = M_{1-}(n, {}^3S_1). \quad (21)$$

In the following, we will study the S-wave top-meson system up to  $n = 4$ . We will calculate both the  $0^-$  and  $1^-$  states and check if they are equal.

### III. NUMERICAL EVALUATION

In order to perform numerical calculations of the BS equation, it is necessary to specify the corresponding parameters. These parameters are determined by fitting the experimental data; that is, they are adjusted such that the calculated meson masses are consistent with the values reported by the Particle Data Group (PDG) [1]. The resulting parameter values are as follows:

$$m_b = 4.960 \text{ GeV}, \quad m_c = 1.620 \text{ GeV}, \quad m_s = 0.500 \text{ GeV}, \quad m_d = 0.311 \text{ GeV}, \\ m_u = 0.305 \text{ GeV}, \quad \alpha_s(m_t) = 0.11, \quad \alpha = 0.06 \text{ GeV}, \quad \lambda = 0.18 \text{ GeV}^2.$$

Based on the formalism and parameters outlined above, we calculate the masses of the  $t\bar{q}$ ,  $t\bar{c}$ , and  $t\bar{b}$  states up to the fourth radial excitation ( $n = 4$ ). The corresponding numerical results are presented in Table I for  ${}^1S_0$  states.

TABLE I: Mass (100 GeV) of  $n^1S_0$  States for Different Quark Combinations

State	$t\bar{b}$	$t\bar{c}$	$t\bar{s}$	$t\bar{d}$	$t\bar{u}$
${}^1S_0$	1.7784	1.7466	1.7364	1.7344	1.7344
${}^2S_0$	1.7813	1.7499	1.7397	1.7376	1.7375
${}^3S_0$	1.7833	1.7521	1.7417	1.7394	1.7393
${}^4S_0$	1.7850	1.7539	1.7432	1.7407	1.7406

From the calculation of the  ${}^3S_1$  states, we find that, for identical quark configurations and principal quantum number  $n$ , the masses of the  ${}^1S_0$  and  ${}^3S_1$  states coincide within our numerical accuracy, which confirms that Eq. (21) is a good approximation.

In the following, we take the  $t\bar{b}$   ${}^1S_0$  state as an example and present its BS wave function explicitly. The BS wave functions for the other states are collected in the Appendix A. From Refs. [62, 63], it can be inferred that, for the  $0^-$  states, the BS

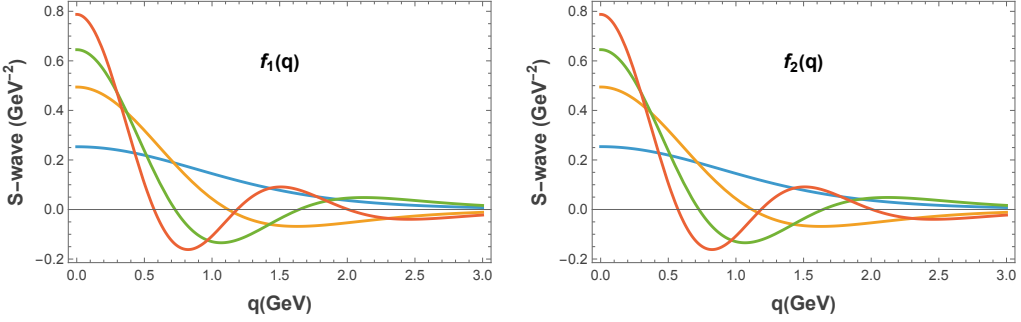


FIG. 1: The BS wave functions for  ${}^1S_0$   $t\bar{b}$  states, blue line for 1S state, orange line for 2S state, green line for 3S state, and red line for 4S state.

wave functions can be decomposed into two parts,  $f_1(q)$  and  $f_2(q)$ . We will next present the curves for  $f_1$  and  $f_2$  of the  ${}^1S_0$  state of the  $t\bar{b}$  system in Fig. 1.

#### IV. POSSIBLE PRODUCTION AND DECAY MODES OF TOPPED MESONS

Within the Standard Model, the lifetime of the top quark is extremely short,

$$\tau_t \simeq \frac{1}{\Gamma_t} \sim 5 \times 10^{-25} \text{ s}, \quad (22)$$

which is much shorter than the typical hadronization timescale,

$$\tau_{\text{had}} \sim 10^{-23} \text{ s}. \quad (23)$$

Therefore, a free top quark decays weakly before it can hadronize into a color-singlet bound state. However, in a boosted frame or in processes where the top quark is produced nearly at rest with respect to an antiquark, the possibility of forming a transient bound state, generally referred to as a topped meson ( $t\bar{q}$ ,  $t\bar{c}$ , or  $t\bar{b}$ ), cannot be completely excluded.

In this section, we present a qualitative analysis of the possible production mechanisms and decay modes of such exotic states.

At hadron colliders such as the LHC, the dominant production mechanisms for top quarks are

$$pp \rightarrow t\bar{t} + X, \quad pp \rightarrow t(\bar{t}) + X, \quad (24)$$

via gluon-gluon fusion and quark-antiquark annihilation.

A topped meson  $T \equiv t\bar{q}$  (or  $t\bar{c}$ ,  $t\bar{b}$ ) may be formed if the produced top quark captures a nearby antiquark before decaying. The possible partonic subprocesses include

$$gg \rightarrow t\bar{t}, \quad t + \bar{q} \rightarrow (t\bar{q}), \quad (25)$$

$$q\bar{q} \rightarrow t\bar{t}, \quad t + \bar{q} \rightarrow (t\bar{q}), \quad (26)$$

$$gb \rightarrow tW^-, \quad t + \bar{b} \rightarrow (t\bar{b}). \quad (27)$$

Among these possibilities, the  $t\bar{b}$  system is expected to have a relatively higher probability of formation due to the heavier mass of the  $\bar{b}$  quark, which leads to a smaller relative velocity and hence a larger overlap of the wave function at the origin.

Qualitatively, the production amplitude can be written as

$$\mathcal{M}(pp \rightarrow T + X) \sim \mathcal{M}(pp \rightarrow t + \bar{q} + X) \psi_T(0), \quad (28)$$

where  $\psi_T(0)$  is the wave function of the bound state at the origin. This implies that compact states such as  $t\bar{b}$  are more favorably produced than  $t\bar{q}$  with  $q = u, d, s$ .

Representative Feynman diagrams for topped meson production include:

- Gluon-gluon fusion: two gluons produce a  $t\bar{t}$  pair, and the  $t$  subsequently binds with a light antiquark from the QCD vacuum.
- Quark-antiquark annihilation:  $q\bar{q} \rightarrow t\bar{t}$ , followed by  $t\bar{q} \rightarrow (t\bar{q})$  binding.
- Associated production:  $gb \rightarrow tW^-$ , with the final  $t$  and  $\bar{b}$  forming a  $(t\bar{b})$  state.

These processes are strongly suppressed by the extremely short lifetime of the top quark, and thus the production cross section of topped mesons is expected to be very small.

Once formed, a topped meson is primarily unstable due to the weak decay of the top quark inside the bound state:

$$t \rightarrow W^+ b. \quad (29)$$

As a result, the dominant decay channel of a topped meson can be written as

$$(t\bar{q}) \rightarrow W^+ + b + \bar{q}. \quad (30)$$

Depending on the decay mode of the  $W^+$  boson, one further obtains

$$(t\bar{q}) \rightarrow \ell^+ \nu_\ell + b + \bar{q}, \quad (31)$$

$$(t\bar{q}) \rightarrow q\bar{q}' + b + \bar{q}. \quad (32)$$

For the  $t\bar{b}$  system, another possible decay channel is

$$(t\bar{b}) \rightarrow W^+ + b + \bar{b}, \quad (33)$$

followed by  $b\bar{b}$  hadronization into bottomonia or bottom-flavored mesons.

In addition, highly excited states may undergo cascade transitions through electromagnetic or strong processes before the weak decay of the top quark, such as

$$(t\bar{q})^* \rightarrow (t\bar{q}) + \gamma, \quad (34)$$

$$(t\bar{q})^* \rightarrow (t\bar{q}) + g, \quad (35)$$

though such transitions are expected to be rare due to the short lifetime of the top quark.

Experimentally, a topped meson event is expected to manifest as an anomalous resonance near the top-quark mass region with final states containing

- a high- $p_T$   $W$  boson,
- one or two  $b$ -jets,
- possibly an additional light jet from the spectator antiquark.

Therefore, the characteristic signal of a topped meson may be summarized as

$$pp \rightarrow T + X \rightarrow W^+ + b + \bar{q} + X, \quad (36)$$

which could, in principle, be distinguished from the standard top decay background by studying specific invariant-mass distributions and angular correlations.

Although the production probability is highly suppressed, a precise analysis at future high-luminosity colliders may still provide hints of such exotic states or impose stringent upper limits on their existence.

## V. SUMMARY

In this work, we investigate the mass spectrum and phenomenological properties of topped mesons, including the  $t\bar{q}$ ,  $t\bar{c}$ , and  $t\bar{b}$  systems, within the framework of the Bethe-Salpeter equation under the instantaneous approximation. We obtain the mass spectra up to the  $n = 4$  states, and our numerical results, presented in Tab. I, show the behavior of the masses for these systems.

Furthermore, we qualitatively analyze the possible production mechanisms and decay patterns of topped mesons at high-energy hadron colliders. Although the extremely short lifetime of the top quark strongly suppresses the formation probability of such bound states, transient topped mesons may still be produced through processes such as gluon fusion or associated production. Once formed, they predominantly decay via the weak decay of the top quark, leading to final states containing a  $W$  boson,  $b$ -jets, and light-flavor jets. These characteristic signatures may provide valuable guidance for future experimental searches at high-luminosity colliders. Our study thus offers a systematic theoretical reference for the exploration of exotic top-flavored bound states.

## Acknowledgments

This work was supported in part by the National Natural Science Foundation of China under Grants 12575106 and 12147214, and Specific Fund of Fundamental Scien-

tific Research Operating Expenses for Undergraduate Universities in Liaoning Province under Grants No. LJ212410165019.

---

- [1] S. Navas and others [Particle Data Group]. Review of particle physics. *Phys. Rev. D*, 110:030001, 2024.
- [2] A. Hayrapetyan and others [CMS]. Observation of a pseudoscalar excess at the top quark pair production threshold. *Rept. Prog. Phys.*, 88:087801, 2025.
- [3] G. Aad and others [ATLAS]. Observation of a cross-section enhancement near the  $t\bar{t}$  production threshold in  $\sqrt{s} = 13$  TeV  $pp$  collisions with the ATLAS detector. *arXiv preprint arXiv:2601.11780*, 2026.
- [4] G. Aad and others [ATLAS]. Observation of quantum entanglement with top quarks at the ATLAS detector. *Nature*, 633:542–547, 2024.
- [5] A. Hayrapetyan and others [CMS]. Observation of quantum entanglement in top quark pair production in proton–proton collisions at  $\sqrt{s} = 13$  TeV. *Rept. Prog. Phys.*, 87:117801, 2024.
- [6] F. J. Llanes-Estrada. Ensuring that toponium is glued, not nailed. *Phys. Lett. B*, 866:139510, 2025.
- [7] J. H. Fu, Y. J. Li, H. M. Yang, Y. B. Li, Y. J. Zhang, and C. P. Shen. Toponium: The smallest bound state and simplest hadron in quantum mechanics. *Phys. Rev. D*, 111:114020, 2025.
- [8] J. H. Fu, Y. J. Zhang, G. Z. Xu, and K. Y. Liu. Toponium: Implementation of a toponium model in FeynRules. *arXiv preprint arXiv:2504.12634*, 2025.
- [9] P. Nason, E. Re, and L. Rottoli. Spin correlations in  $t\bar{t}$  production and decay at the LHC in QCD perturbation theory. *JHEP*, 10:149, 2025.
- [10] J. Ellis. Personal memories of 50 years of quarkonia. *Nucl. Phys. B*, 1018:117062, 2025.
- [11] H. S. Shao and G. Wang. Analytic NNLO transverse-momentum-dependent soft function for heavy quark pair hadroproduction at threshold. *JHEP*, 10:164, 2025.
- [12] C. Xiong and Y. J. Zhang. Probing Yoctosecond Quantum Dynamics in Toponium

Formation at Colliders. *arXiv preprint arXiv:2507.05703*, 2025.

[13] E. J. Thompson. Top Quark Bound States in Finite and Holomorphic Quantum Field Theories. *arXiv preprint arXiv:2507.16831*, 2025.

[14] Aman Desai, Amelia Lovison, and Paul Jackson. Analysing Toponium at the LHC using Recursive Jigsaw Reconstruction. *arXiv preprint arXiv:2601.19187*, 1 2026.

[15] Aman Desai, Amelia Lovison, and Paul Jackson. Reconstructing Toponium using Recursive Jigsaw Reconstruction. In *18th International Workshop on Top Quark Physics (TOP2025)*, 1 2026.

[16] Thomas Flacke, Benjamin Fuks, Dongchan Kim, Jinheung Kim, Seung J. Lee, and Léandre Munoz-Aillaud. New physics in toponium's shadow? *arXiv preprint arXiv:2512.03220*, 12 2025.

[17] Z. Rajabi Najjar and K. Azizi. Masses of Purely Top-Quark Bound States: Toponium and the Triply-Top Baryon. *arXiv preprint arXiv:2511.10053*, 11 2025.

[18] Benjamin Fuks, Aminul Hossain, and James Keaveney. Statistical indications of toponium formation in top quark pair production. *Phys. Lett. B*, 873:140179, 2026.

[19] Benjamin Fuks, Kaoru Hagiwara, Kai Ma, Léandre Munoz-Aillaud, and Ya-Juan Zheng. Prospects for toponium formation at the LHC in the single-lepton mode. *arXiv preprint arXiv:2509.03596*, 9 2025.

[20] Victor P. Goncalves, Luana Santana, and Bruno D. Moreira. Exclusive vector toponium photoproduction in hadronic collisions. *Eur. Phys. J. C*, 85(12):1443, 2025.

[21] Chang Xiong and Yu-Jie Zhang. Probing Yoctosecond Quantum Dynamics in Toponium Formation at Colliders. *arXiv preprint arXiv:2507.05703*, 7 2025.

[22] Jing-Hang Fu, Yu-Ji Li, Hui-Min Yang, Yu-Bo Li, Yu-Jie Zhang, and Cheng-Ping Shen. Toponium: The smallest bound state and simplest hadron in quantum mechanics. *Phys. Rev. D*, 111(11):114020, 2025.

[23] Nosheen Akbar, Ishrat Asghar, and Zaki Ahmad. Mass Spectrum, Radii, and Radiative Decay Widths of Toponium. *arXiv preprint arXiv:2411.08548*, 11 2024.

[24] Yueling Yang, Bingbing Yang, Jiazhi Li, Zhaojie Lu, and Junfeng Sun. Searching for the toponium  $\eta_t$  with the  $\eta_t \rightarrow \mathbf{W}^+ \mathbf{W}^-$  decay\*. *Chin. Phys.*, 50(3):033101, 2026.

[25] Y. Bai, T. K. Chen, and Y. Yang. Toponia at the HL-LHC, CEPC, and FCC-ee. *arXiv preprint arXiv:2506.14552*, 2025.

[26] S. Hirata. Neutral current effects for  $e^+e^-$  annihilation in to  $\mu^+\mu^-$  in the toponium region. *Prog. Theor. Phys.*, 64:342, 1980.

[27] V. S. Fadin and V. A. Khoze. Threshold Behavior of Heavy Top Production in e+ e- Collisions. *JETP Lett.*, 46:525–529, 1987. LENINGRAD-87-1333.

[28] A. Djouadi, J. Ellis, and J. Quevillon. Contrasting pseudoscalar Higgs and toponium states at the LHC and beyond. *Phys. Lett. B*, 866:139583, 2025.

[29] S. W. Zhang, X. Luo, H. M. Yang, and H. X. Chen. QCD sum rule study of topped mesons within heavy quark effective theory. *Universe*, 11:10, 2025.

[30] S. W. Zhang, W. H. Tan, X. Luo, and H. X. Chen. Topped baryons from QCD sum rules. *arXiv preprint arXiv:2507.05895*, 2025.

[31] S. Q. Luo, Q. Huang, and X. Liu. The quest for topped hadrons. *arXiv preprint arXiv:2508.17646*, 2025.

[32] J. A. Aguilar-Saavedra. Toponium hunter’s guide. *Phys. Rev. D*, 110:054032, 2024.

[33] S. J. Jiang, B. Q. Li, G. Z. Xu, and K. Y. Liu. Study on Toponium: Spectrum and Associated Processes. *arXiv preprint arXiv:2412.18527*, 2024.

[34] A. Jafari. TOP2024: an overview of experimental results. *arXiv preprint arXiv:2501.16231*, 2025.

[35] G. L. Wang, T. F. Feng, and Y. Q. Wang. Mass spectra and wave functions of toponia. *Phys. Rev. D*, 111:096016, 2025.

[36] R. Francener, V. P. Goncalves, and D. E. Martins. Investigating the exclusive toponium production at the LHC and FCC. *arXiv preprint arXiv:2502.03295*, 2025.

[37] V. S. Fadin and V. A. Khoze. Threshold behavior of heavy top production in  $e^+e^-$  collisions. *JETP Letters*, 46:525–529, 1987. LENINGRAD-87-1333.

[38] J. H. Kuhn and P. M. Zerwas. The toponium scenario. *Physics Reports*, 167:321, 1988.

[39] V. D. Barger, E. W. N. Glover, K. Hikasa, W. Y. Keung, M. G. Olsson, C. J. Suchyta, and X. R. Tata. Superheavy quarkonium production and decays: A new higgs signal. *Physical Review D*, 35:3366, 1987. Erratum: *Phys. Rev. D* 38, 1632 (1988).

[40] M. J. Strassler and M. E. Peskin. The heavy top quark threshold: Qcd and the higgs. *Physical Review D*, 43:1500–1514, 1991.

[41] V. S. Fadin, V. A. Khoze, and T. Sjostrand. On the threshold behavior of heavy top production. *Zeitschrift für Physik C*, 48:613–622, 1990.

[42] V. S. Fadin, V. A. Khoze, and M. I. Kotsky. Top quark polarization as a probe of  $t\bar{t}$  threshold dynamics. *Zeitschrift für Physik C*, 64:45–56, 1994.

[43] A. H. Hoang, M. Beneke, K. Melnikov, T. Nagano, A. Ota, A. A. Penin, A. A. Pivovarov, A. Signer, V. A. Smirnov, Y. Sumino, et al. Top–anti-top pair production close to threshold: Synopsis of recent nnlo results. *Eur. Phys. J. direct*, 2(1):3, 2000.

[44] K. Hagiwara, Y. Sumino, and H. Yokoya. Bound-state effects on top quark production at hadron colliders. *Physics Letters B*, 666:71–76, 2008.

[45] A. A. Penin, V. A. Smirnov, and M. Steinhauser. Heavy quarkonium spectrum and production/annihilation rates to order  $\beta_0^3\alpha_s^3$ . *Nuclear Physics B*, 716:303–318, 2005.

[46] Y. Sumino and H. Yokoya. Bound-state effects on kinematical distributions of top quarks at hadron colliders. *Journal of High Energy Physics*, 09:034, 2010. Erratum: JHEP 06, 037 (2016).

[47] Y. Kiyo, J. H. Kuhn, S. Moch, M. Steinhauser, and P. Uwer. Top-quark pair production near threshold at lhc. *European Physical Journal C*, 60:375–386, 2009.

[48] M. Beneke, Y. Kiyo, P. Marquard, A. Penin, J. Piclum, and M. Steinhauser. Next-to-next-to-next-to-leading order qcd prediction for the top antitop *s*-wave pair production cross section near threshold in  $e^+e^-$  annihilation. *Physical Review Letters*, 115(19):192001, 2015.

[49] S. Kawabata and H. Yokoya. Top-quark mass from the diphoton mass spectrum. *European Physical Journal C*, 77(5):323, 2017.

[50] J. Reuter, B. C. Nejad, A. Hoang, W. Kilian, M. Stahlhofen, T. Teubner, and C. Weiss. Exclusive top threshold matching at lepton colliders. In *Proceedings of Science*, volume ICHEP2018 of *PoS*, page 654, 2019.

[51] B. Fuks, K. Hagiwara, K. Ma, and Y. J. Zheng. Signatures of toponium formation in lhc run 2 data. *Physical Review D*, 104(3):034023, 2021.

[52] J. A. Aguilar-Saavedra. Toponium hunter's guide. *Physical Review D*, 110(5):054032, 2024.

[53] D. d'Enterria and K. Kang. Exclusive photon-fusion production of even-spin resonances and exotic qed atoms in high-energy hadron collisions. *arXiv preprint arXiv:2503.10952*, 2025.

[54] M. V. Garzelli, G. Limatola, S. O. Moch, M. Steinhauser, and O. Zenaiev. Updated predictions for toponium production at the lhc. *Physics Letters B*, 866:139532, 2025.

[55] G. L. Wang, T. F. Feng, and Y. Q. Wang. Mass spectra and wave functions of toponia. *Physical Review D*, 111(9):096016, 2025.

[56] B. Fuks, K. Hagiwara, K. Ma, and Y. J. Zheng. Simulating toponium formation signals at the lhc. *European Physical Journal C*, 85(2):157, 2025.

[57] E. E. Salpeter, H. A. Bethe, E. E. Salpeter, D. Lurie, C. Itzykson, and J. B. Zuber. Phys. Rev. 84, 1232(1951); Phys. Rev. 87, 328(1952); Particles and Fields (Wiley,1968); Quantum Field Theory (McGraw-Hill,1980). Miscellaneous references.

[58] J. D. Stack, S. Otto, J. D. Stack, D. Barkai, et al. Phys. Rev. D**29**, 1213 (1984); Phys. Rev. Lett.**52**, 2328 (1984); Phys. Rev. D **30**, 1293 (1984). Miscellaneous references.

[59] A. Huntley, C. Michael, and C. Michael. Nucl. Phys. B**286**, 211 (1987); Phys. Rev. Lett.**56**, 1219(1986). Miscellaneous references.

[60] C. f. Qiao, H. W. Huang, and K. T. Chao. Possible retardation effects of quark confinement on the meson spectrum. *Phys. Rev. D*, 54:2273–2278, 1996.

[61] E. Laermann, others, and K. D. Born. Phys. Lett. B**173**, 437 (1986); Phys. Rev. D**40**, 1653 (1989). Miscellaneous references.

[62] Jin-Mei Zhang and Guo-Li Wang. Strong Decays of the Radial Excited States  $B(2S)$  and  $D(2S)$ . *Phys. Lett. B*, 684:221–223, 2010.

[63] C. S. Kim and Guo-Li Wang. Average kinetic energy of heavy quark  $(\mu(\pi)^{**2})$  inside heavy meson of 0- state by Bethe-Salpeter method. *Phys. Lett. B*, 584:285–293, 2004. [Erratum: Phys.Lett.B 634, 564 (2006)].

## Appendix A: The BS wave functions for $^1S_0$ states

The BS wave functions for  $^1S_0$   $t\bar{c}$ ,  $t\bar{s}$ ,  $t\bar{d}$ , and  $t\bar{u}$  are shown in Figs. 2-5

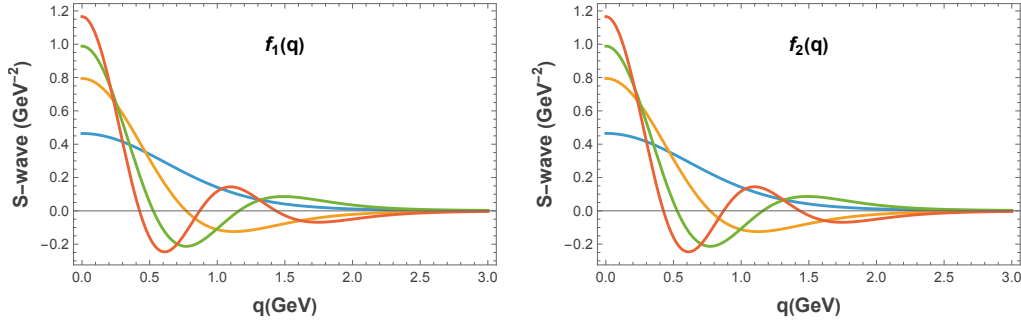


FIG. 2: The BS wave functions for  $^1S_0$   $t\bar{c}$  states, blue line for 1S state, orange line for 2S state, green line for 3S state, and red line for 4S state.

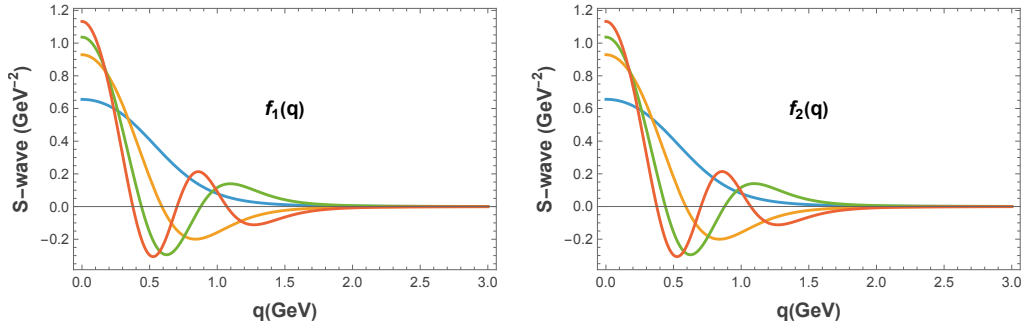


FIG. 3: The BS wave functions for  $^1S_0$   $t\bar{s}$  states, blue line for 1S state, orange line for 2S state, green line for 3S state, and red line for 4S state.

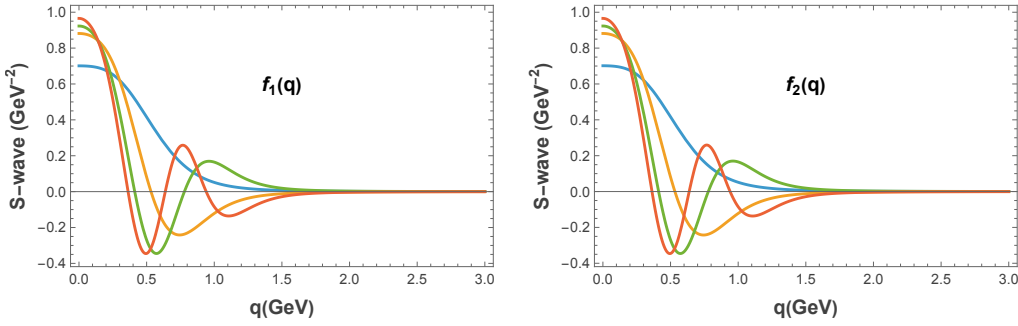


FIG. 4: The BS wave functions for  $^1S_0$   $t\bar{d}$  states, blue line for 1S state, orange line for 2S state, green line for 3S state, and red line for 4S state.

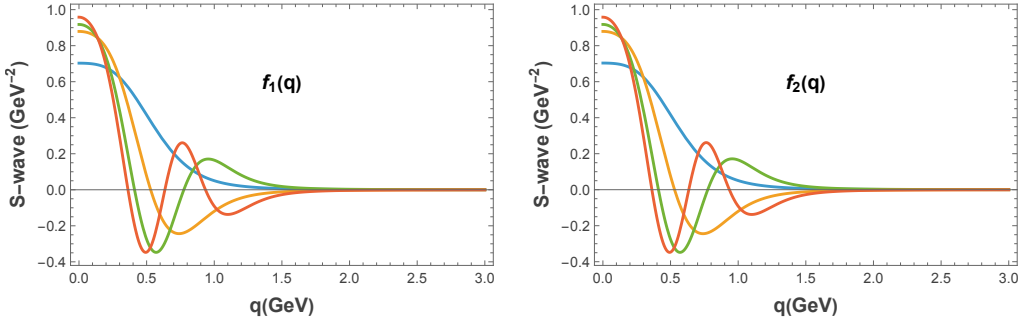


FIG. 5: The BS wave functions for  $^1S_0$   $t\bar{u}$  states, blue line for 1S state, orange line for 2S state, green line for 3S state, and red line for 4S state.